Convection in a Conditionally Unstable Atmosphere: A Re-investigation of BJERKNES' Slice Method

J. Oerlemans

Institute of Meteorology and Oceanography, University of Utrecht, Princetonplein 5, Utrecht, The Netherlands

(Manuscript received 04.04.1985, in revised form 25.09.1985)

Abstract:

A general formulation of the buoyancy budget in a horizontal slice, in the middle of a conditionally unstable atmosphere, permits a comparison of various convection patterns, and provides a natural extension of BJERKNES' (1938) theory. Here we consider centre-up, centre-down, and roll patterns. Lateral entrainment between up- and downdraught region is assumed to consist of two parts: background mixing and mixing induced by the convective motions themselves. Due to the latter nonlinearity, finite-amplitude convection is possible.

Linear stability analysis of the state of rest shows that the centre-up pattern is the most unstable configuration. Non-zero steady states are also compared. It turns out that the centre-down pattern has the smallest amplitude, while the centre-up pattern 'performs best'. The results suggest that a centre-down pattern can only persist when background mixing is small. This agrees with the fact that open cells, qualitatively similar to the centre-down pattern analysed here, are normally found over homogeneous water surfaces when wind shear is not too large.

Several authors have suggested that maximizing the upward heat flux can be used to determine a preferred horizontal length scale for convection. The results presented here cast some doubt on the applicability of such an extremal principle, because open cells, so frequently observed in reality, have the smallest upward heat flux.

Zusammenfassung: Konvektion in einer bedingt labilen Atmosphäre: eine erneute Untersuchung der BJERKNES'schen „slice" Methode

Eine allgemeine Formulierung der Haushaltsgleichungen bei thermischer Konvektion in einer horizontalen Schicht inmitten einer bedingt labilen Atmosphäre erlaubt einen Vergleich verschiedener Konvektions-Anordnungen und führt zu einer natürlichen Erweiterung der Theorie von BJERKNES (1938). Wir betrachten hier Anordnungen zentrierter Aufwärts- und Abwärtsbewegungen und Rollen-Strukturen. Das seitliche Entrainment zwischen den Gebieten mit positiver und negativer Vertikalbewegung bestehe aus zwei Anteilen: den überlagerten Mischungsprozessen und dem Austausch, der durch die konvektiven Bewegungen selber hervorgerufen wird. Der damit verbundenen Nichtlinearität entspricht die Konvektion mit endlicher Amplitude.

Eine lineare Stabilitätsanalyse im Ruhezustand zeigt, daß die zentrierte Aufwärtsbewegung die labilste Konfiguration darstellt. In den von Null verschiedenen stationären Zuständen zeigt die Anordnung mit Abwärtsbewegung die kleinste Amplitude, während die mit Aufwärtsbewegung „sich am besten verhält". Die Ergebnisse zeigen Persistenz der Abwärtsbewegung wenn die überlagerten Mischungsprozesse klein sind. Dies stimmt damit überein, daß offene Zellen normalerweise über homogenen Wasseroberflächen bei nicht zu starker Windscherung beobachtet werden.

Verschiedene Autoren haben vermutet, daß die Maximierung des nach oben gerichteten Wärmestromes dazu benutzt werden kann, eine bevorzugte horizontale Längenskala für die Konvektion zu bestimmen. Die hier vorliegenden Ergebnisse lassen Zweifel an einem derartigen Extremalprinzip aufkommen, weil offene Zellen (die so häufig in der Natur beobachtet werden) den kleinsten nach oben gerichteten Wärmefluß besitzen.

0005-8173/86/01 0041–13 $ 03.00/0

Résumé: Convection dans une atmosphère conditionellement instable. Réanalyse de la méthode en couche de Bjerknes

Une formulation générale du bilan de poussée dans une couche horizontale, au centre d'une atmosphère conditionnellement instable, permet une comparaison de diverses configurations convectives et procure une extension naturelle de la théorie de BJERKNES (1938). On considère des configurations avec mouvements ascendants, descendants et en rouleaux. On admet que l'entraînement latérale entre les régions d'ascendance et de subsidence comporte deux contributions: un mélange avec l'environnement et un mélange induit par les mouvements convectifs eux-mêmes. En raison de la non linéarité de ces derniers, un mouvement convectif d'amplitude finie est possible.

Une analyse linéaire de la stabilité de l'état de repos montre que la configuration avec mouvement ascendant au centre est la plus instable. Des états stationnaires non nuls sont également analysés. Il apparaît que c'est la configuration avec mouvement descendant au centre qui a la plus faible amplitude tandis que c'est la configuration avec ascendance qui se développe le mieux. Les résultats suggèrent que le mouvement subsident ne peut se maintenir que si le mélange avec l'environnement est faible. Ceci est en accord avec le fait que les cellules ouvertes, qualitativement semblables aux mouvements centraux subsidents analysés ici, se rencontrent le plus souvent au-dessus de surfaces marines homogènes, lorsque le cisaillement du vent n'est pas trop grand.

Plusieurs auteurs ont suggéré que l'on pouvait utiliser la méthode qui consiste à rendre le flux vertical de chaleur maximum pour déterminer une échelle horizontale préférentielle pour la convection. Les résultats obtenus jettent un doute sur le bien fondé de ce principe d'extremum puisque les cellules ouvertes, si souvent observées, ont le flux de chaleur le plus faible.

1 Introduction

In the atmosphere, long-lasting convection in an absolutely unstable layer is rare. It is only in cases of strong solar heating of very dry air over land, or just after cold continental air hits a warm sea, that absolutely unstable conditions dominate. In most cases the atmosphere is conditionally unstable, i. e. unstable for moist ascent and stable for dry ascent (and descent).

In a conditionally unstable atmosphere convection leads to heating in both the updraught region (through latent heat release) and the downdraught region (adiabatic heating). It is the difference in the heating rates that determines the buoyancy, and thus the generation of kinetic energy. One of the consequences is that the relative size of the up- and downdraught areas has to obey certain conditions for convective instability to occur. Such conditions were already formulated by BJERKNES (1938) and PETTERSSEN (1939). By means of the so-called slice method they showed that on the average available potential energy is generated only when the area with upward motion is less than the area with downward motion times $(\gamma - \gamma_s)/(\gamma_a - \gamma)$. Here γ_a is the dry adiabatic, γ_s the moist and γ the actual lapse rate.

The stabilizing effect of compensating downward motions has also been studied with much more complicated numerical models of convective clouds (e. g. OGURA, 1963; ASAI and KASAHARA, 1967). Such studies have shown that downward motions are of extreme importance, even on short time scales.

At present times, in studies of atmospheric convection BJERKNES' slice method has been replaced by numerical models. Nevertheless, some further investigation of the simple 'buoyancy budget model' is possible. Studying convection by just looking at the buoyancy budget in a horizontal slice, somewhere in the middle of the convective layer, has its limitations, of course. In such an approach it is hardly possible to deal with the effects of shear of the background wind, growth of the convective layer, and, in particular, variations in the vertical structure of the convective disturbance. Looking at the buoyancy budget at one level is in fact equivalent to considering a first mode in the vertical only. That a stability analysis with an extremely simple prescribed vertical structure works was for example shown by RAY-

LEIGH (1916): although convection naturally starts off with highly asymmetric and local thermals, a theory based on a prescribed (wavy) vertical dependence of velocity and temperature appears to be able to predict when thermal instability sets in (namely, at the critical RAYLEIGH number). Another example is provided by analytic studies on linear baroclinic instability (e. g. PEDLOSKY, 1979). These facts encouraged the author to re-investigate BJERKNES' slice method.

Two conditions are at the basis of applying the buoyancy budget in a horizontal slice to study convection, namely:

(i) the atmosphere is conditionally unstable, and shearing of the background wind is small;
(ii) the dynamics of the convection have a substantially smaller characteristic time scale than those of the background flow.

Condition (i) implies that the convective motions have to draw the major part of their energy from latent heat release, whereas condition (ii) makes it possible that the convective system can be in internal balance (generation of kinetic energy on the convective scale by buoyancy forces equals dissipation by mixing, while the statistical properties of the convection are determined by the large-scale variables).

The conditions described above are frequently met over the tropical oceans, but can sometimes also been found in 'older' polar outbreaks when thermal forcing from below becomes smaller and wind shear weakens. For an example see BAKAN (1982), who discusses a case of persistent open-cell convection over the North Sea with only a 1 K air-sea temperature difference and little shear.

In this paper, the basic equations for the slice method are formulated in a more general way, making it possible to study the effect of the geometry of the convective elements. The influence of horizontal entrainment of momentum and heat on the stability of various convection patterns can then be studied. We will consider centre-up, centre-down, and roll patterns.

A number of authors have used an extremal principle (maximizing the net upward heat flux) to derive a preferred spatial scale of the convective disturbance (e. g. KUO, 1961; ASAI and KASAHARA, 1967). Numerical experimentation on two-dimensional convection lends some support to the applicability of an extremal principle of this kind (for a discussion on this matter, see ASAI, 1983). If maximizing the upward heat flux would determine the scale of convective elements, it should also be possible to obtain information about the geometry: when the principle is of real physical significance, the convection pattern with the largest heat flux should be the preferred mode. The approach taken in this paper offers the possibility to study this point in a simple way.

This paper proceeds as follows. In Section 2 the model equations are derived, starting from the incompressible Boussinesq approximation. The essential step is averaging of the momentum and thermodynamic equations over the up- and downdraught regions (for axial symmetry, this procedure has been described by ASAI and KASAHARA, 1967). Special care is taken in formulating the horizontal entrainment. The mixing coefficient is split into a background part, to deal with the degree of turbulence in the air mass of consideration, and a part determined by the intensity of the convection. The stability of the state of rest is discussed in Section 3, while non-zero steady states are investigated in Section 4.

A summary of the results of the model, together with some examples (satellite pictures and soundings) illustrating its applicability, are found in the last section.

2 Basic Equations

The slice method of studying atmospheric convection is essentially based on the assumption that a 'level of symmetry' exists, i.e. that vertical gradients in mean (that is, non-turbulent) quantities vanish at some height. In the absence of shear of the horizontal wind, the equations for the slice, which is assumed to be advected with the horizontal wind, take a simple form.

It is assumed that for the present schematic model the equations for shallow, incompressible flow can be used. They read (e. g. DUTTON, 1976):

$$\left(\frac{\partial}{\partial t} + \vec{v}\cdot\nabla\right)\vec{v} = -\frac{\theta'}{T_m}\vec{g}, \tag{1}$$

$$\left(\frac{\partial}{\partial t} + \vec{v}\cdot\nabla\right)\frac{\theta'}{T_m} + \frac{w}{T_m}\frac{\partial \theta_p}{\partial z} = \frac{1}{c_p}\frac{ds}{dt} \tag{2}$$

$$\nabla\cdot\vec{v} = 0 \tag{3}$$

Here $\vec{v}$ is air velocity, T_m an overall reference temperature, θ' perturbation temperature, $\vec{g}$ gravitational acceleration, w upward velocity, $\theta_p(z)$ reference potential temperature, c_p specific heat and s entropy. Note that a pressure perturbation term does not occur because the convective layer is assumed to be shallow.

It is common practice in studies of moist convection to replace the diabatic heating term by a procedure in which prescribed lapse rates are applied for ascending and descending motion. To obtain convenient equations the followings steps/assumptions have to be applied:

- neglect the divergence of vertical fluxes (the symmetry condition), i. e. apply the equations to the 'middle' of the convective layer.
- decompose the wind and temperature field in a mean and fluctuating part ($\vec{v} = \bar{\vec{v}} + \vec{v}'$; $\theta = \bar{\theta} + \theta'$)
- average the resulting equations over the updraught area U and the downdraught area D (see Figure 1)
- neglect the shear in the horizontal background wind and advect the system with the mean horizontal wind

The equations then read:

$$\frac{\partial \overline{w}_U}{\partial t} + \frac{1}{U}\int_U \nabla_2\cdot\vec{v}_2' \, w' \, dU = \frac{g}{T_m}(\bar{\theta}_U - \theta_0), \tag{4}$$

$$\frac{\partial \overline{w}_D}{\partial t} + \frac{1}{D}\int_D \nabla_2\cdot\vec{v}_2' \, w' \, dD = \frac{g}{T_m}(\bar{\theta}_D - \theta_0), \tag{5}$$

$$\frac{\partial \bar{\theta}_U}{\partial t} + \frac{1}{U}\int_U \nabla_2\cdot\vec{v}_2' \, \theta' \, dU = (\gamma - \gamma_s)\,\overline{w}_U, \tag{6}$$

$$\frac{\partial \bar{\theta}_D}{\partial t} + \frac{1}{D}\int_D \nabla_2\cdot\vec{v}_2' \, \theta' \, dD = (\gamma - \gamma_a)\,\overline{w}_D, \tag{7}$$

$$\overline{w}_U \, U + \overline{w}_D \, D = 0. \tag{8}$$

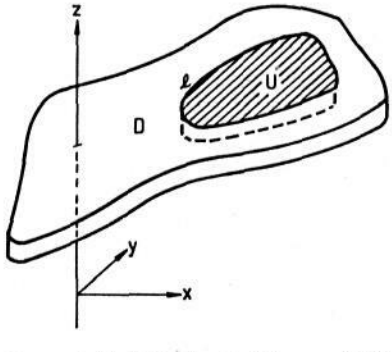

Figure 1
Geometry for the slice model. The slice is considered as a level of symmetry (zero divergence of vertical fluxes)

Equation (8) follows from the assumption that the horizontally-averaged vertical wind vanishes. The indices U and D refer to up- and downdraught, the index 2 to horizontal flow (i.e. in the slice). The overbar indicates a mean value over the relevant area, e.g.:

$$\overline{w}_U = \frac{1}{U}\int_U w\, dU.$$

Lapse rates for moist and dry vertical motion are indicated by γ_s and γ_a, respectively. The environmental temperature, relevant to the buoyancy forces, is denoted by θ_0.

The second terms in (4) and (5) represent the lateral eddy fluxes, as can be seen by applying Gauss' theorem:

$$\frac{1}{U}\int_U \nabla_2 \cdot \vec{v}'_2\, w'\, dU = \frac{1}{U}\int_l \vec{v}'_{2n}\, w'\, dl \equiv \frac{l}{U}\langle \vec{v}'_{2n}\, w' \rangle, \text{ where} \tag{9}$$

$$\langle \ldots \rangle = \frac{1}{L}\int_l \ldots\, dl \tag{10}$$

In (9), $\vec{v}'_{2n}$ is the perturbation velocity perpendicular to the boundary l of the updraught/downdraught system, which has length L. We assume that the lateral eddy fluxes, or entrainment, can be handled by K-theory, so we write:

$$\langle \vec{v}'_{2n}\, X' \rangle = K(\overline{X}_U - \overline{X}_D) \tag{11}$$

The factor of proportionality K needs some further discussion. It should in fact include a mixing length squared, divided by a horizontal length scale typical for the updraught/downdraught system. However, the problem we face here is that in convection in a conditionally unstable atmosphere quantities like vertical motion do not change smoothly when going from the centre of the updraught to the centre of the downdraught area. Instead, gradients are generally large and concentrated at the cloud edges. This implies that it makes little sense to relate either the mixing length or the characteristic horizontal length scale to the areas of updraught and downdraught regions. We therefore assume the existence of an intrinsic length scale, independent of U and D, that determines K. We will allow K to depend only on the difference in vertical motion in the up- and downdraught regions.

In this approach, (4) and (5) take the form.

$$\frac{\partial \overline{w}_U}{\partial t} = \frac{g}{T_m}(\overline{\theta}_U - \theta_0) - K'_m(\overline{w}_U - \overline{w}_D)\frac{L}{U}, \tag{12}$$

$$\frac{\partial \overline{w}_D}{\partial T} = \frac{g}{T_m}(\overline{\theta}_D - \theta_0) - K'_m(\overline{w}_D - \overline{w}_U)\frac{L}{D} \tag{13}$$

Similar equations are easily written down for $\overline{\theta}_U$ and $\overline{\theta}_D$, where the entrainment coefficient K'_m for momentum has to be replaced by the entrainment coefficient K'_h for heat. They read

$$\frac{\partial \overline{\theta}_U}{\partial t} = (\gamma - \gamma_s)\overline{w}_U - K'_h(\overline{\theta}_U - \overline{\theta}_D)\frac{L}{U} \tag{14}$$

$$\frac{\partial \overline{\theta}_D}{\partial t} = (\gamma - \gamma_a)\overline{w}_D - K'_h(\overline{\theta}_D - \overline{\theta}_U)\frac{L}{D} \tag{15}$$

Together with the continuity Equation (8), (12)–(15) form a set of 5 equations in the unkowns θ_0, $\overline{w}_U$, $\overline{w}_D$, $\overline{\theta}_U$, $\overline{\theta}_D$. θ_0 can be obtained directly by multiplying (12) by U and multiplying (13) by D and adding the resulting equations. With (8) it then follows that

$$\theta_0 = (U\overline{\theta}_U + D\overline{\theta}_D)/(U + D) \tag{16}$$

This is a consistent result. It should be stressed at this point that we consider U and D as parameters to be specified. Further manipulation of the equations leads to two equations in $\overline{w}_U$ and $\overline{\theta}_U - \overline{\theta}_D$:

$$(1 + U/D)\frac{dw}{dt} = \frac{g}{T_m}\Delta - K'_m (1 + U/D)(L/U + L/D)\, w, \tag{17}$$

$$\frac{d\Delta}{dt} = \left[\gamma - \gamma_s + (\gamma - \gamma_a)\frac{U}{D}\right] w - K'_h (L/U + L/D)\, \Delta. \tag{18}$$

where

$$w = \overline{w}_U, \quad \Delta = \overline{\theta}_U - \overline{\theta}_D.$$

It should be noted that lateral fluxes through the outer boundary of the downdraught region have been set to zero. The reason for this will become clear later, when the choice of convection patterns implies symmetry conditions at this boundary.

According to the discussion above, the exchange coefficient depends on the up- and downdraught velocities. However, it should also include a constant part, so we write

$$K'_i = K_i (1 + \alpha |\overline{w}_U - \overline{w}_D|) = K_i [1 + \alpha(1 + U/D)\, w], \tag{19}$$

where the index i is either m (momentum) or h (heat). K_i reflects the 'background mixing', and therefore characterizes the air mass in which the convection occurs. The parameter α determines how the exchange coefficient increases when convection develops. Note that this increase is necessary to allow finite-amplitude solutions of the present model ! Furthermore, it is assumed that the dependence of K_i on $|\overline{w}_U - \overline{w}_D|$ is the same for heat and momentum.

Inserting (19) in (17) and (18) finally leads to the set of equations to be analyzed. They read

$$\frac{dw}{dt} = \frac{g/T_m}{1 + U/D}\Delta - K_m [1 + \alpha(1 + U/D)\, w]\, (L/U + L/D)\, w, \tag{20}$$

$$\frac{d\Delta}{dt} = \left[\gamma - \gamma_s + (\gamma - \gamma_a)\frac{U}{D}\right] w - K_h [1 + \alpha(1 + U/D)\, w]\, (L/U + L/D)\, \Delta. \tag{21}$$

It is obvious that to this set of equations the constraint $w \geqslant 0$ should be added. So, in summary, we have derived two equations for the updraught velocity w and the temperature difference Δ, with γ, K_m, K_h and α as model constant. How L is related to U and D depends on the geometry, i. e. on the convection pattern.

3 Stability Analysis

We first introduce the parameters $q_1, q_2, q_3, p_1, p_2, p_3$ to allow a shorter notation when desired:

$$q_1 = \frac{g/T_m}{1 + U/D}, \qquad p_1 = \left[\gamma - \gamma_s + (\gamma - \gamma_a)\frac{U}{D}\right],$$

$$q_2 = K_m L\left(\frac{1}{U} + \frac{1}{D}\right), \qquad p_2 = K_h L\left(\frac{1}{U} + \frac{1}{D}\right), \tag{22}$$

$$q_3 = K_m \alpha L(1 + U/D)\left(\frac{1}{U} + \frac{1}{D}\right), \qquad p_3 = K_h \alpha L(1 + U/D)\left(\frac{1}{U} + \frac{1}{D}\right).$$

So (20) and (21) can be rewritten as

$$\frac{dw}{dt} = q_1 , \Delta - q_2 \, w - q_3 \, w^2 , \tag{23}$$

$$\frac{d\Delta}{dt} = p, w - p_2 \, \Delta - p_3 \, \Delta w. \tag{24}$$

Note that all parameters except p_1 are always positive. Although in principle the set (23)–(24) can have periodic solutions, this in fact prohibited a priori by the constraint $w \geqslant 0$.

The following steady states are now found:

$$\text{(i)} \quad w = 0, \quad \Delta = 0 \tag{25}$$

$$\text{(ii)} \quad w = -\frac{1}{2}\left(\frac{p_2}{p_3} + \frac{q_2}{q_3}\right) \pm \frac{1}{2}\left[\left(\frac{p_2}{p_3} + \frac{q_2}{q_3}\right)^2 - 4\,\frac{p_2\, q_2}{p_3\, q_3} + 4\,\frac{p_1\, q_1}{p_3\, q_3}\right]^{1/2}$$

$$\Delta = \frac{q_2}{q_1} w + \frac{q_3}{q_1} w^2$$

Since w should be positive, only the + sign in (ii) applies. So the system has at most two real solutions with physical meaning, one of which is the state of rest. We will now examine under what conditions this state is unstable.

Linearizing around the state of rest, the amplification matrix is found to be

$$\begin{pmatrix} -q_2 & q_1 \\ p_1 & -p_2 \end{pmatrix}$$

from which it follows that at least one eigenvalue is positive when

$$-\frac{1}{2}(K_m + K_h)\, L\left(\frac{1}{U} + \frac{1}{D}\right) + \tag{26}$$

$$+\frac{1}{2}\sqrt{L^2\left(\frac{1}{U} + \frac{1}{D}\right)^2 (K_h - K_m)^2 + \frac{4g/T_m}{1 + U/D}\left[\gamma - \gamma_s + (\gamma - \gamma_a)\frac{U}{D}\right]} \quad > 0.$$

Generally speaking, a larger scale of the convective elements, i. e. larger values of U and D, favours instability of the state of rest. So, as expected, large U and D allows the convection to overcome the destructive force of entrainment. Condition (26) also shows that linear growth rates will be larger if the eddy Prandtl number $Pr\,(\equiv K_m/K_h)$ deviates from unity.

Before investigating the neutral stability curves for various convection patterns, we note that with $K_m = K_h = 0$ (26) reduces to

$$\frac{U}{D} < \frac{\gamma - \gamma_s}{\gamma_a - \gamma} \tag{27}$$

This condition was already discussed by BJERKNES (1938), and simply implies that convection develops when heating in the updraught exceeds heating in the downdraught.

We now consider three 'modes', as shown in Figure 2. Shading corresponds to upward motion. As basic area we take a square, which, according to the definitions of U and D, has sides of length $(U + D)^{1/2}$. The convective patterns associated with these modes are such that there exists symmetry with respect to the sides of the square. This also justifies the assumption made earlier, namely that fluxes through the outer boundary of the slice (see Figure 1) are zero.

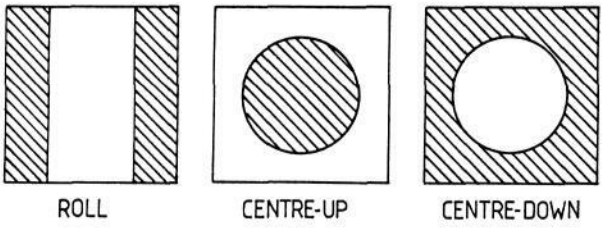

• **Figure 2**
The three configurations of convection considered in this study. The area of the basic square is U+D. The regions of upward motion are shaded.

For the modes shown in Figure 2 the values of L are immediately found:

for the roll pattern: $L = 2\sqrt{U + D}$,

for the centre-up pattern: $L = 2\sqrt{\pi U}$,

for the centre-down pattern: $L = 2\sqrt{\pi D}$,

Using these expressions for L in (26), it is now possible to construct the neutral stability curves.

Some examples are shown in Figure 3. Updraught area U and downdraught area D are plotted on logarithmic scales. Curves are given for rather stable conditions ($\gamma = 7$ K/km) and rather unstable conditions ($\gamma = 9.6$ K/km). Generally, a centre-up pattern is the most unstable structure, followed by the roll pattern and centre-down pattern. It is only for large values of the lapse rates (close to γ_a), that regions in the U, D-plane exist where the roll and centre-down patterns are the only unstable structures. These regions are small, however.

The structure of the stability diagram hardly depends on the entrainment coefficients K_m and K_h, that is, the relative location of the neutral curves of the various modes is not sensitive to these parameters. Of course, for instability to occur larger values of U and D are required when K_m and/or K_h are increased.

KRISHNAMURTI (1975), in a completely different analysis of convection, discusses the importance of the eddy PRANDTL number Pr, and what values of Pr are actually found in the atmosphere. The resulting suggestion is that Pr is in the 1 to 50 range, with a tendency for small values to occur near the earth's surface, and larger values higher up in the atmosphere. An example of neutral curves for Pr = 25 is shown in Figure 3c. The values of γ and K_m were not changed, so Figure 3c is comparable to Figure 3b. Because K_h is thus reduced by a factor 25, instability of the state of rest now occurs for smaller values

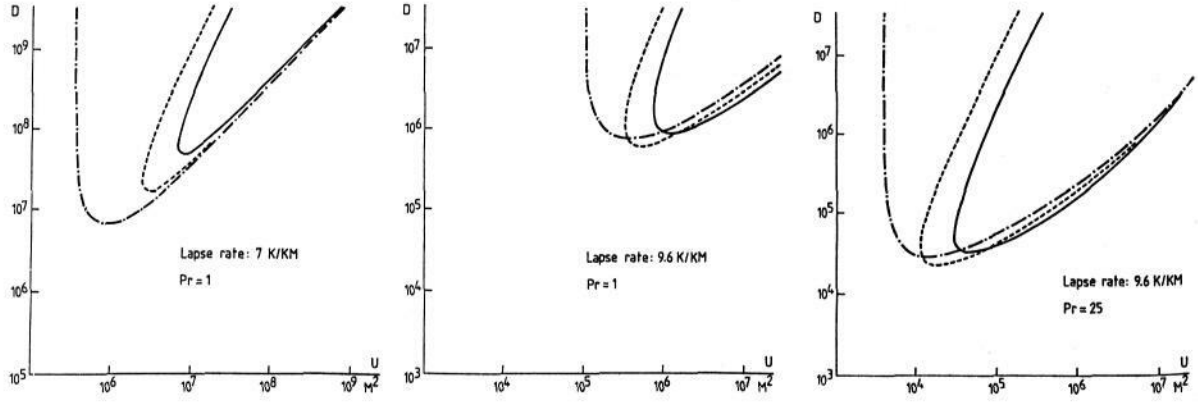

• **Figure 3** Neutral stability curves for the roll (– – – –), the centre-down (——) and the centre-up pattern (–·–·), as a function of updraught area U and downdraught area D. Parameter values: $K_m = 1$ m/s, $\gamma_a = 10$ K/km, $\gamma_s = 6$ K/km.

of U and D. However, the relative position of the neutral curves for the three convection patterns is virtually unchanged.

A similar stability analysis can be carried out for the nonzero steady state in (25), but it is not necessary to perform this. The equilibria were obtained by solving the cubic equation in w, which resulted from eliminating Δ between (23) and (24). This cubic equation has the structure of the elementary cusp catastrophe, and $w = 0$ is either the only or the intermediate solution (when three equilibria exist). Exchange of stability is therefore granted (e. g. GILMORE, 1981). So when $w = 0$ becomes unstable, the other solutions (we are only interested in the positive one, in fact) become stable, and vice versa. The nonzero steady states of relevance are thus stable within the neutral curves displayed in Figure 3. In the next section we have a closer look at these steady states.

4 Steady States

The nonzero steady states can be calculated directly from (25). Although the stability properties of the solutions do not depend on α (q_3 and p_3 do not appear in the amplification matrix), the amplitude does, of course. Here we chose $\alpha = 10$ s/m, giving realistic amplitudes.

Because we want to compare geometric patterns, U + D (the total area of the basic square) is now prescribed. The natural quantity to vary then is R = D/U (note that this is not the aspect ratio in its normal definition). An example is shown in Figure 4a. The updraught velocity is shown as a function of R, for U + D = 100 km^2 and $\gamma = 8$ K/km. It is quite obvious that centre-up patterns have the largest amplitude. Centre-down patterns have the smallest amplitude and rolls are found in between. This picture is typical: using other values of α, γ, U + D, etc. effects the amplitude (for example, for more stable conditions amplitudes are smaller), but not in an essential way the ranking of the modes.

As discussed in the Introduction, maximizing the upward heat flux has been used as an extremal principle to determine the horizontal length scale or aspect ratio (horizontal extent of a convective element divided by its vertical extent). ASAI (1983) provides an overview on this matter. This principle has only been used for two-dimensional (vertical plane) convection. The present analysis allows to investigate whether such a principle can also be used to select the geometric pattern in plan view.

The upward heat flux through the slice is

$$F = \frac{U\bar{\theta}_U\bar{w}_U + D\bar{\theta}_D\bar{w}_D}{U+D} = \frac{Uw\Delta}{U+D} \tag{28}$$

Values of F corresponding to the w-amplitudes discussed above are shown in Figure 4b. The curves show a much more pronounced maximum, and the centre-up pattern turns out to be the most efficient

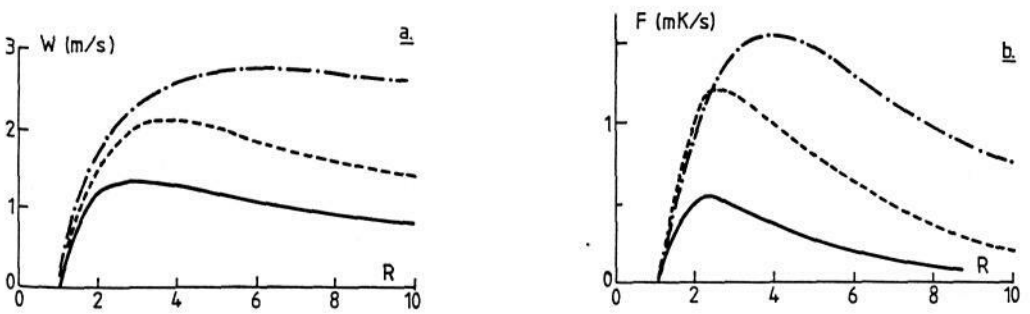

Figure 4 Steady-state values of w (a) and corresponding upward heat flux (b), as a function of R (= D/U). The different curves are for roll (– – – –), centre-down (_____) en centre-up (—·—·) pattern. Parameter values: $K_m = 1$ m/s, Pr = 25, $\alpha = 4$ s/m, $\gamma_a = 10$ K/km, $\gamma_s = 6$ K/km, $\gamma = 8$ K/km, U+D = 10^8 m^2.

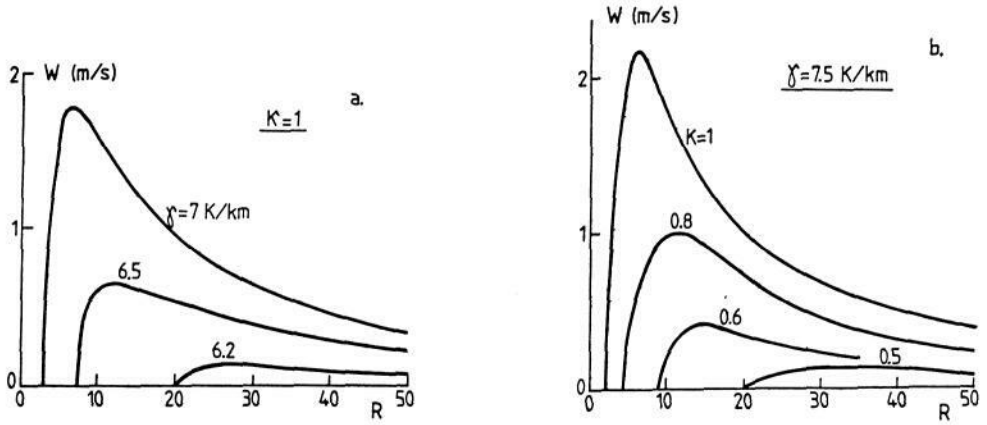

Figure 5 Steady-state values of w, as a function of R, for various values of γ (lapse rate) and γ (cloud depth). All curves are for the centre-down pattern. In a γ is varied and K = 1. In b K is varied while γ = 7.5 K/km. Other parameter values are as in Figure 4, except U+D = $9 \cdot 10^8$ m^2.

structure. Since open cell patterns, which are qualitatively similar to the centre-down pattern, are so common, it seems that they cannot be explained as being the most effective mode to transport heat upwards, casting doubt on the applicability of this extremal principle. We return to this in the discussion.

Because open cell patterns occur so frequently, we investigate them in some more detail. Figure 5a shows w as a function of R for some values of the lapse rate γ. The graphs reveal how the amplitude decreases and R should increase (to keep the convection going) when conditions become more stable. These graphs are for a basic square of 30 to 30 km, with other parameter values as used previously.

Another way in which convection may be suppressed in an air mass is by decreasing relative humidity. To mimic the effect of humidity on the condensation level, an effective cloud depth κ is introduced, normalized by the total depth of the convective layer. So, there is moist ascent over κ and dry ascent over $(1-\kappa)$. The parameter p_1 in (22) should thus be replaced by

$$p_1 = \kappa\,(\gamma - \gamma_s) + (1 - \kappa + U/D)\,(\gamma - \gamma_a) \tag{29}$$

Note that now the buoyancy budget should be interpreted as a vertical mean rather than a local one. Figure 5b shows some amplitude curves calculated with (29). The strong effect of decreasing cloud depth is obvious, and, as expected, very similar to the effect of increasing stability of the stratification. Some further inferences on the basis of these results will be made in the Discussion.

5 Discussion

In this paper convection in a conditionally unstable atmosphere has been studied by extending the well-known slice method of BJERKNES (1938). The buoyancy budget in the slice has been formulated in more general terms, allowing a calculation of the buoyancy for any geometric pattern. Also, a more refined treatment of entrainment was included by splitting the mixing coefficient in a background part and a 'convectively induced' part. The resulting system of equations appeared to have two equilibria: the state of rest and finite-amplitude convection, one state being stable when the other one is unstable. Starting from a state of rest and increasing the size of the convective elements, it turned out that the centre-up pattern is the first mode to grow. The centre-down pattern requires the largest forcing to be able to grow. An analysis of the steady states revealed that the centre-up pattern is the first mode to grow. The centre-down pattern requires the largest forcing to be able to grow. An analysis of the steady

states revealed that the centre-up pattern is the most effective structure in transporting heat upwards, while the centre-down pattern performs least and the roll pattern is in between.

So far, this theory is a straightforward and a natural extension of BJERKNES' approach, and demonstrates in a relatively simple way how entrainment and the geometric pattern determine whether convection in a conditionally unstable atmosphere may persist or not. In the preceding sections not much reference has been made to observations, but of course some inferences can be made.

A first thing to note is that, when considering finite amplitude convection, the centre-up pattern is best protected against lateral entrainment, whereas the centre-down pattern is least. So if the background mixing (i. e. the level of turbulence in the air mass considered) is large, one cannot expect a persistent centre-down pattern. It is not surprising then, that the centre-down pattern is preferably found over sea in cases where shearing of the horizontal wind is small. Such situations are typically found over the tropical oceans and in polar outbreaks in a mature stage. Although many workers consider latent heat release to be a secondary effect in the dynamics of convection in polar outbreaks, some indication exists that this point of view is not always correct.

An example of a polar outbreak over the North Atlantic is shown in Figure 6. As soon as the cold air mass hits the warm sea, rolls form. Here thermal instability in RAYLEIGH's sense (absolutely unstable stratification) and wind shear are without doubt the most important factors. In a later stage the rolls evolve to open cells (north of the region where strong subsidence prevents growth of the convective layer and leads to overcast). Here cloudiness decreases and R (= D/U) increases. This picture is typical, see e. g. WALTER (1980).

It frequently happens that in a northwesterly flow over the North Sea region air masses arrive that have been subject to heating during one or even two days. Open cells with large cross section and large values of U/D are then observed, while average cloudiness is in fact very small ($\simeq 0.2$). In such cases wind shear is insignificant (except close to the surface) and the lapse rate is slightly greater than the moist adiabat.

Figure 6

NOAA-7 satellite picture of a polar outbreak over the North Atlantic Ocean (4 November 1982). Note the general transition from rolls to cells, the increase in size of the convective elements, and the decrease in cloudiness (all in downstream direction.

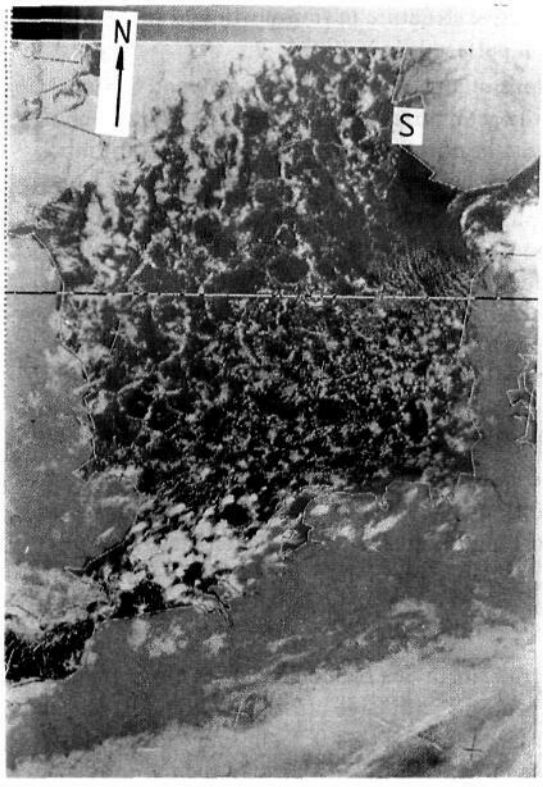

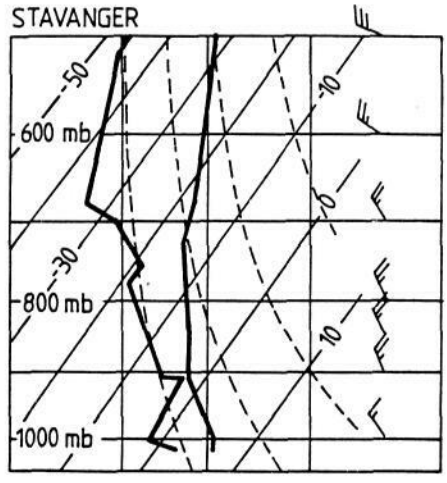

Figure 7

NOAA infared picture of open cells over the North Sea, 28 October 1983, 18 : 48 UT. The sounding at Stavanger (Norway, indicated in the photograph) at 12 : 00 UT is also shown. In the diagram, vertical lines are moist-adiabats, dashed lines adiabats, and sloping lineas isotherms (Labelled in °C). Note the advection of cold air around 600 mb, the very small wind shear below this level, and the fairly stable stratification.

An example is shown in Figure 7. The location of the sounding is indicated in the photograph. It is quite obvious that in this case the convection has to be driven by latent heat release. Similar situations are frequently seen over the western Atlantic, with ever increasing values (downstream) of D/U. In view of the results from the model presented in this paper, this should be interpreted as an attempt of the convection to survive while the stratification stabilizes and humidity goes down.

Over land, cases with rather homogeneous polar air having little wind shear and sufficient moisture are rare, so it is not surprising that normally rolls and centre-up patterns are encountered. A few examples exist, however, of centre-down patterns over land with a horizontal scale comparable to those observed over the oceans. One is shown in Figure 8. Convection over central Europe has organised itself into an open cellular pattern. Note that wind shear is really very small, and that the lapse rate is only slightly unstable for moist ascent.

It is difficult to state in general when latent heat release becomes the primary force for driving convection. In most cases convection starts by the creation of an absolutely unstable lapse rate. Thermal instability then occurs and the upward heat flux rapidly stabilizes the stratification (shown in the simplest fashion by LORENZ, 1963). Latent heat release then comes into play, and convection may continue as long as moisture is available. The present theory is meant to describe this stage, where an internal buoyancy balance exists with slowly varying external factors like lapse rate and moisture content.

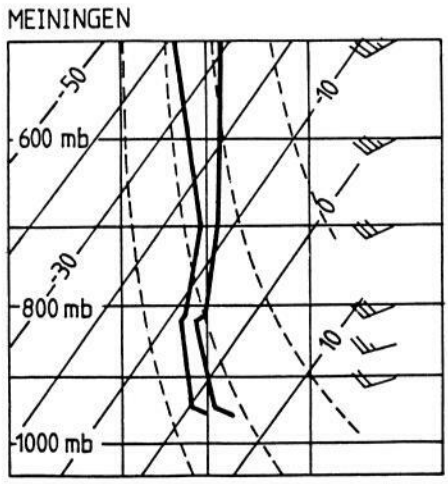

Figure 8

NOAA infrared picture of open cells over central Europe. The North Sea is in the upper left corner, and the snow-covered Alps are found near the bottom.
Date: 27 March 1984, 14:23 UT. Also shown is the sounding at Meiningen (Germany, indicated in the photograph). See Figure 7 for explanation of the diagram. Note that the wind shear is very small, and that only a very thin layer close to the surface is superadiabatic.

References

ASAI, T., 1983: On the preferred mode of cumulus convection in a conditionally unstable atmosphere. In: Cloud Dynamics (Eds.: E. M. AGEE, T. ASAI), Terra (Tokyo) & Reidel (Dordrecht), 149–162.

ASAI, T. and KASAHARA, A., 1967: A theoretical study of the compensating downward motions associated with cumulus clouds. J. Atmos. Sci. **24**, 487–496.

BAKAN, S., 1982: Open cellular structures during KonTur. In: KonTur, Convection and Turbulence Experiment, Preliminary Scientific Results, Univ. of Hamburg, 51–62.

BJERKNES, J., 1938: Saturated ascent of air through a dry-adiabatically descending environment. Quart. J. Roy. Met. Soc. **64**, 325–330.

DUTTON, J. A., 1976: The Ceaseless Wind. McGraw-Hill (New York), 579 pp.

GILMORE, R., 1981: Catastrophe Theory for Scientists and Engineers. J. Wiley & Sons (New York), 666 pp.

KRISHNAMURTI, R., 1975: On cellular cloud patterns. Part 3: applicability of the mathematical and laboratory models. J. Atmos. Sci. **32**, 1373–1383.

KUO, H. L., 1961: Convection in conditionally unstable atmosphere. Tellus **13**, 441–459.

LORENZ, E. N., 1963: Deterministic nonperiodic flow. J. Atmos. Sci. **20**, 130–141.

OGURA, Y., 1963: The evolution of a moist convective element in a shallow, conditionally unstable atmosphere. J. Atmos. Sci. **20**, 407–424.

PEDLOSKY, J., 1979: Geophysical Fluid Dynamics. Springer (New York), 624 pp.

PETTERSSEN, S., 1939: Contributions to the theory of convection. Geofys. Publ. **12**, 5–23.

RAYLEIGH, Lord, 1916: On convection currents in a horizontal layer of fluid when the higher temperature is on the under side. Phil. Mag. **6**, 529–546.

WALTER, B. A., 1980: Wintertime observations of roll clouds over the Bering Sea. Mon. Wea. Rev. **108**, 2024–2031.